Supplementary Information

A Robust and Efficient Heterogeneous MoS_2/Al_2O_3 Catalyst for the Hydrogenative Recycling of Polyurethane Waste

Congxue Yuan,[a] Shuang Cao,[a] Liang Chen,[a] Ruitong Gao,*[a] Yajing Duan*[b] and Hui Du*[a]

[a]College of Chemistry and Chemical Engineering, Qingdao University, Qingdao, Shandong, 266071, P. R. China.
E-mail: gaoruitong@qdu.edu.cn, duhui@qdu.edu.cn
[b]College of Physics, Qingdao University, Qingdao, Shandong 266071, P. R. China.
E-mail: duanyajing@qdu.edu.cn

Supplementary Tables

Table S1. The ICP-OES elemental analysis of MoS_2/Al_2O_3.

Sample	element	Content (%)
	S	4.67
MoS_2/Al_2O_3	Mo	6.71
	Al	21.70

Table S2. The average molecular weight of **PU-1**.

Peak	Rt min	M_p g/mol	M_n g/mol	M_w g/mol	M_z g/mol	M_{z+} g/mol	PDI
1	8.240	16960	8235	22098	45289	74003	2.683424

Table S3. Comparison of catalysts for PU hydrogenation reported in recent literature.

PU model	Catalyst	Reaction conditions	Product	Ref.
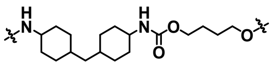 **M_w unknown** **1 mmol**	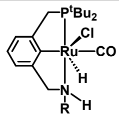 **R = ^{t}Bu R= Benzyl** **0.02 mmol**	**KO^{t}Bu (0.08 mmol), DMSO, H_2 (70 bar), 150 °C, 48 h**	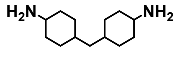 **66%** 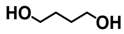 **70%**	**1**
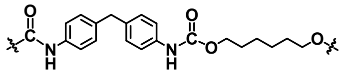 **M_w unknown** **1 mmol**	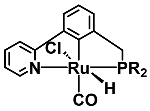 **R = Cy** **1 mol%**	**KO^{t}Bu (4 mol%), THF, H_2 (50 bar), 120 °C, 24 h**	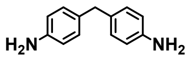 **76%** 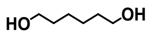 **85%**	**2**
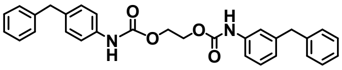 **0.5 mmol**	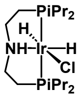 **1 mol%**	**KO^{t}Bu (2 mol%), THF, H_2 (30 bar), 150 °C, 21 h**	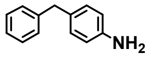 **93%** 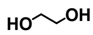 **not detected**	**3**
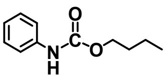 **0.5 mmol**	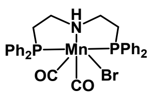 **2 mol%**	**KO^{t}Bu (6 mol%), toluene/*i*PrOH, 120 °C, 16 h**	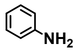 **79%** 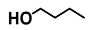 **62%**	**4**
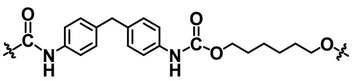 **M_w unknown** **1 mmol**	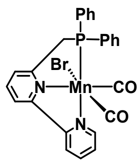 **0.04 mmol**	**KO^{t}Bu (0.08 mmol), toluene, H_2 (60 bar), 170 °C, 24 h**	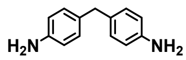 **81%** 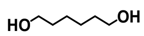 **79%**	**5**
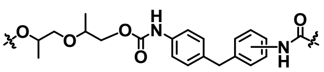 **M_w unknown** **260 mg**	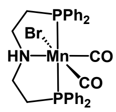 **1 wt%**	**KOH (10 wt%), *i*PrOH, H_2 (50 bar), 180 °C, 21 h**	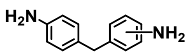 **92%** 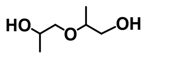 **92%**	**6**
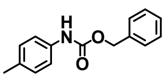 **2 mmol**	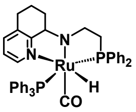 **0.25 mol%**	**KBH_4 (0.25 mol%), *tert*-amyl alcohol, H_2 (50 bar), 140 °C, 20 h**	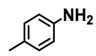 **98%** 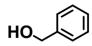 **95%**	**7**
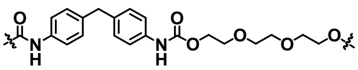 **M_w ~33 kDa** **200 mg**	**ZnO-ZrO_2/Cu** **200 mg**	**THF (30 mL), CO_2/H_2 (1/3, v/v, 3 MPa), 200 °C, 4 h**	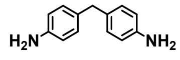 **~25.0%** 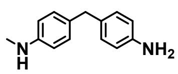 **~61.4%** 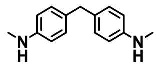 **~16.7%** 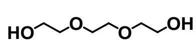	**8**

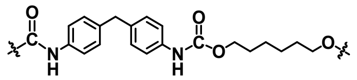 **M_w unknown** **300 mg**	**NiMo/γ-Al_2O_3** **100 mg**	**KOH (6 wt%), 1,4-dioxane, H_2 (50 bar), 185 °C, 16 h**	**~99.8%** 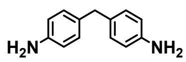 **92%** 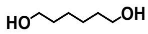 **not detected**	**9**
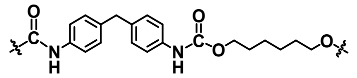 **M_w ~1.3 kDa** **250 mg**	**CeO_2** **25 mg**	**H_2 (10 bar), 200 °C, 4 h**	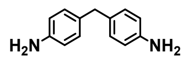 **89%** 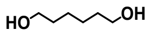 **97%**	**10**
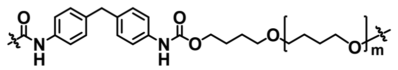 **M_w ~181 kDa** **3.3 g**	**Pd/γ-Al_2O_3** **10 wt%**	**KBH_4 (1 wt%), *tert*-amyl alcohol, H_2 (50 bar), 180 °C, 24 h**	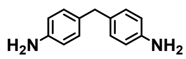 **0.54 g** 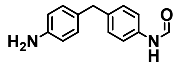 **0.35 g** 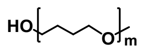 **Mw ~3.5 kDa**	**11**
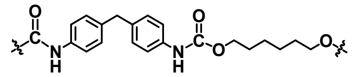 **M_w ~22 kDa** **300 mg**	**MoS_2/Al_2O_3** **50 mg**	**K_2CO_3 (15 mg), 1,4-dioxane, H_2 (50 bar), 185 °C, 12 h**	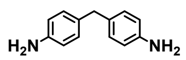 **84.2%** 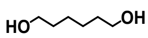 **92.5%**	**This work**

Table S4. Supplemental experiments on the catalytic performance of MoS_2/Al_2O_3.

Entry	Reactant	Catalyst	Aniline yield (%)
1[a]	1,3-Diphenylurea	50 mg MoS_2/Al_2O_3	72.5
2[a]	1,3-Diphenylurea	50 mg MoS_2/Al_2O_3 + 15 mg K_2CO_3	98.7

a: Reaction conditions: 173 mg of 1,3-Diphenylurea, catalyst (specific amount as indicated in the table), 5 mL of 1,4-dioxane, 185 °C, 50 bar H_2, 600 rpm, 4 h.

Table S5. Life Cycle Assessment (LCA) calculation data of the MoS_2/Al_2O_3 system.

	GWP kgCO_2-Eq	FAETP kg1,4-DCB-Eq	NREU MJ	HTP kg1,4-DCB-Eq	ADP kgSb-Eq
PU	5.2967	0.0818	88.8417	4.5308	4.81E-05
H_2	0.0297	0.0023	1.7420	0.0231	1.43E-08
Al_2O_3	0.0170	0.0004	0.2491	0.0051	1.75E-08
MoO_3	0.0157	0.0013	0.1633	0.0629	4.47E-05
S powder	0.0001	0.0000	0.0018	0.0001	1.55E-11
K_2CO_3	0.0155	0.0002	0.1764	0.0156	1.78E-07
Energy	0.0006	0.0000	0.0050	0.0008	1.20E-09
Waste	0.4462	0.0069	7.4849	0.3817	4.05E-06
Aromatic amine	-0.8766	-0.0072	-21.2104	-0.9672	-8.36E-06
Polyol	-2.2547	-0.0149	-44.1899	-0.1621	-5.30E-07
Methanol	-0.0351	-0.0017	-1.5690	-0.0079	-8.52E-08
Total	2.6551	0.0691	31.6946	3.8828	8.81E-05

Note: The environmental impacts were assessed for five impact categories using the CML (v4.8 2016 no LT) method: Global Warming Potential (GWP) (kgCO_2-Eq), Freshwater Aquatic Ecotoxicity Potential (FAETP) (kg1,4-DCB-Eq), Non-Renewable Energy Use (NREU) (MJ), Human Toxicity Potential (HTP) (kg1,4-DCB-Eq), and Abiotic Depletion Potential (ADP) (kgSb-Eq). Based on published reports, the target product yield was assumed to be comparable across the catalytic systems evaluated.[9, 11] Therefore, the functional unit was defined as 1 kg of PU. The catalyst was assumed to be used for 10 cycles.

Table S6. LCA calculation data of the NiMo/γ-Al_2O_3 system.

	GWP kgCO_2-Eq	FAETP kg1,4-DCB-Eq	NREU MJ	HTP kg1,4-DCB-Eq	ADP kgSb-Eq
PU	5.2967	0.0818	88.8417	4.5308	4.81E-05
H_2	0.0297	0.0023	1.7420	0.0231	1.43E-08
$(NH_4)_6Mo_7O_{24}\cdot 4H_2O$	0.0784	0.0066	0.8167	0.3148	2.24E-04
$Ni(NO_3)_2\cdot 6H_2O$	0.0331	0.0338	0.4123	0.1479	4.02E-06
S powder	0.0008	0.0000	0.0101	0.0004	8.81E-11
γ-Al_2O_3	0.0235	0.0005	0.3441	0.0071	2.42E-08
KOH	0.0160	0.0002	0.1872	0.0145	1.73E-07
Energy	0.0008	0.0000	0.0064	0.0010	1.53E-09
Waste	0.4462	0.0069	7.4849	0.3817	4.05E-06
Aromatic amine	-0.8766	-0.0072	-21.2104	-0.9672	-8.36E-06
Polyol	-2.2547	-0.0149	-44.1899	-0.1621	-5.30E-07
Methanol	-0.0351	-0.0017	-1.5690	-0.0079	-8.52E-08
Total	2.7588	0.1083	32.8758	4.2840	2.71E-04

Table S7. LCA calculation data of the Pd/γ-Al_2O_3 system.

	GWP kgCO_2-Eq	**FAETP kg1,4-DCB-Eq**	**NREU MJ**	**HTP kg1,4-DCB-Eq**	**ADP kgSb-Eq**
PU	5.2967	0.0818	88.8417	4.5308	4.81E-05
H_2	0.0297	0.0023	1.7420	0.0231	1.43E-08
$Pd(NO_3)_2·2H_2O$	5.6116	0.1325	78.6834	3.6162	3.77E-04
γ-Al_2O_3	0.0112	0.0002	0.1638	0.0034	1.15E-08
KOH	0.0027	0.0000	0.0312	0.0024	2.88E-08
Energy	0.0012	0.0001	0.0092	0.0014	2.20E-09
Waste	0.4462	0.0069	7.4849	0.3817	4.05E-06
Aromatic amine	-0.8766	-0.0072	-21.2104	-0.9672	-8.36E-06
Polyol	-2.2547	-0.0149	-44.1899	-0.1621	-5.30E-07
Methanol	-0.0351	-0.0017	-1.5690	-0.0079	-8.52E-08
Total	8.2328	0.2000	109.9868	7.4217	4.20E-04

Supplementary Figures

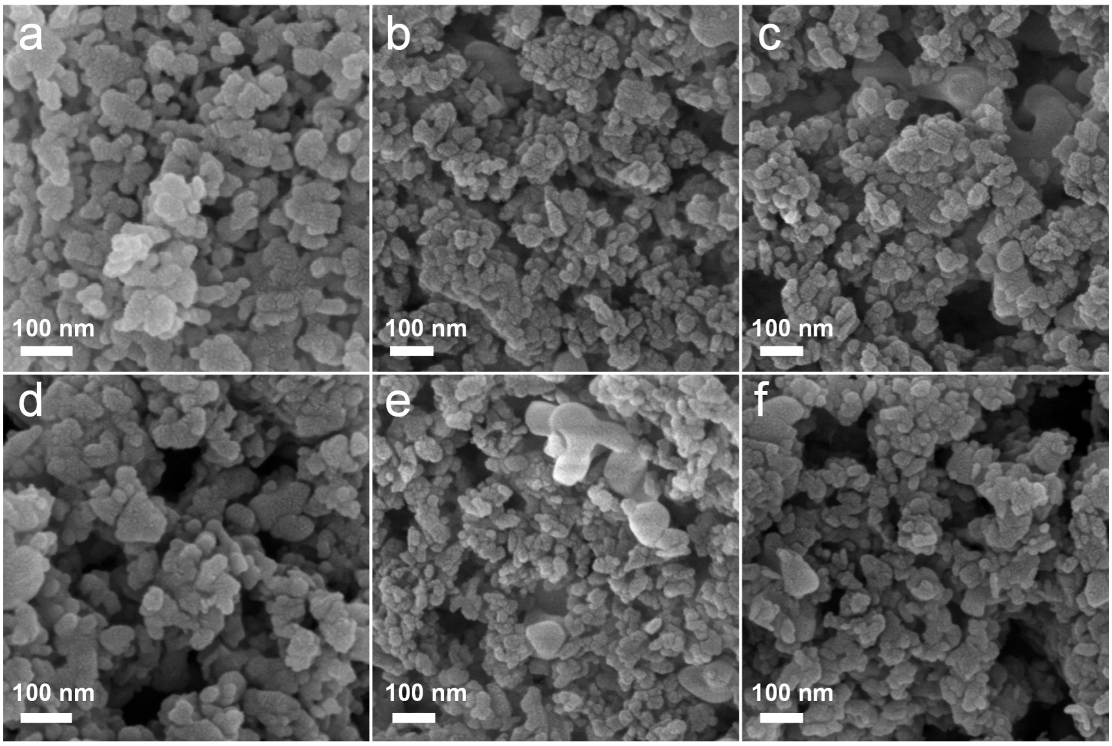

Fig. S1 SEM images of Al_2O_3 (**a–c**) and MoS_2/Al_2O_3 (**d–f**).

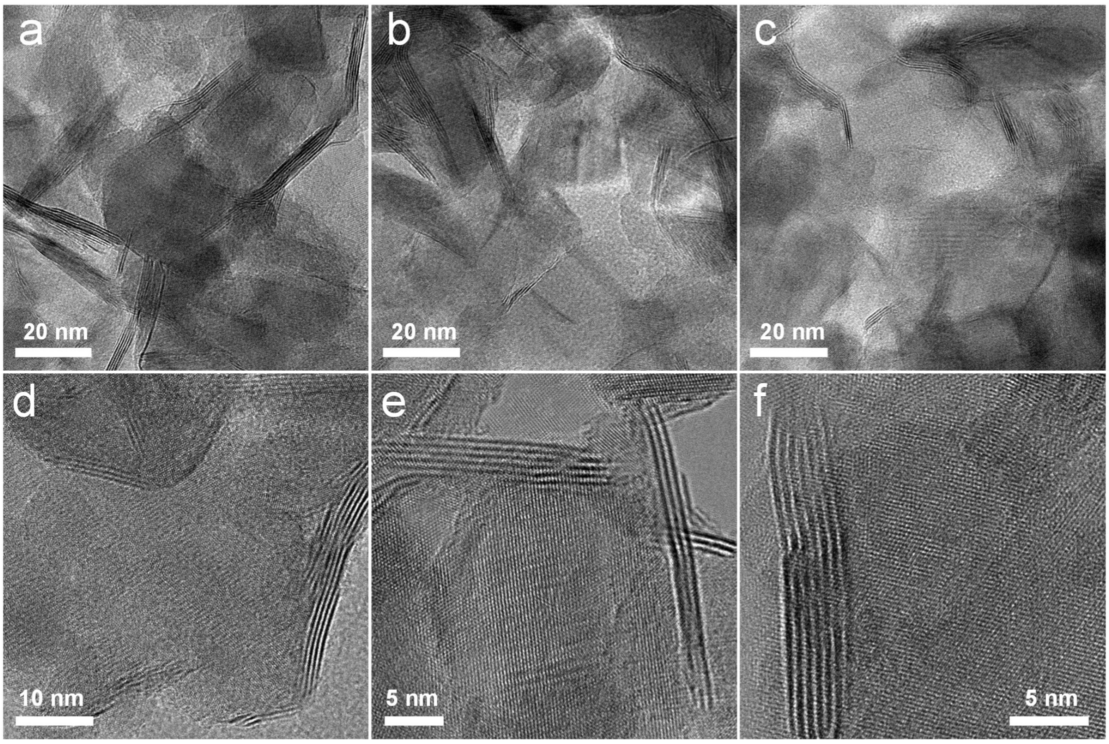

Fig. S2 HR-TEM images of MoS_2/Al_2O_3 (**a–f**).

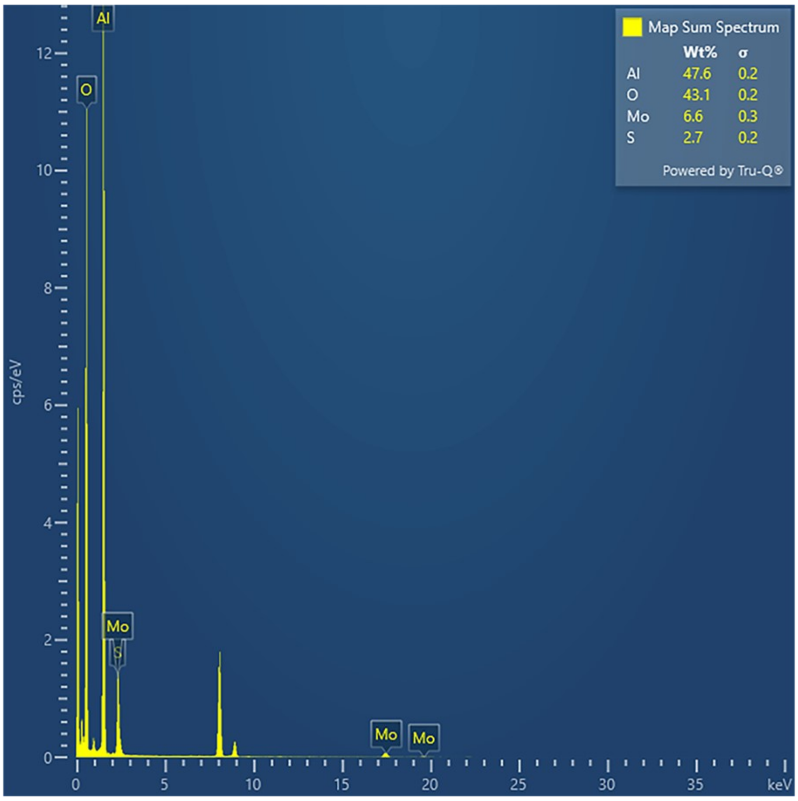

Fig. S3 EDS spectrum of the MoS_2/Al_2O_3.

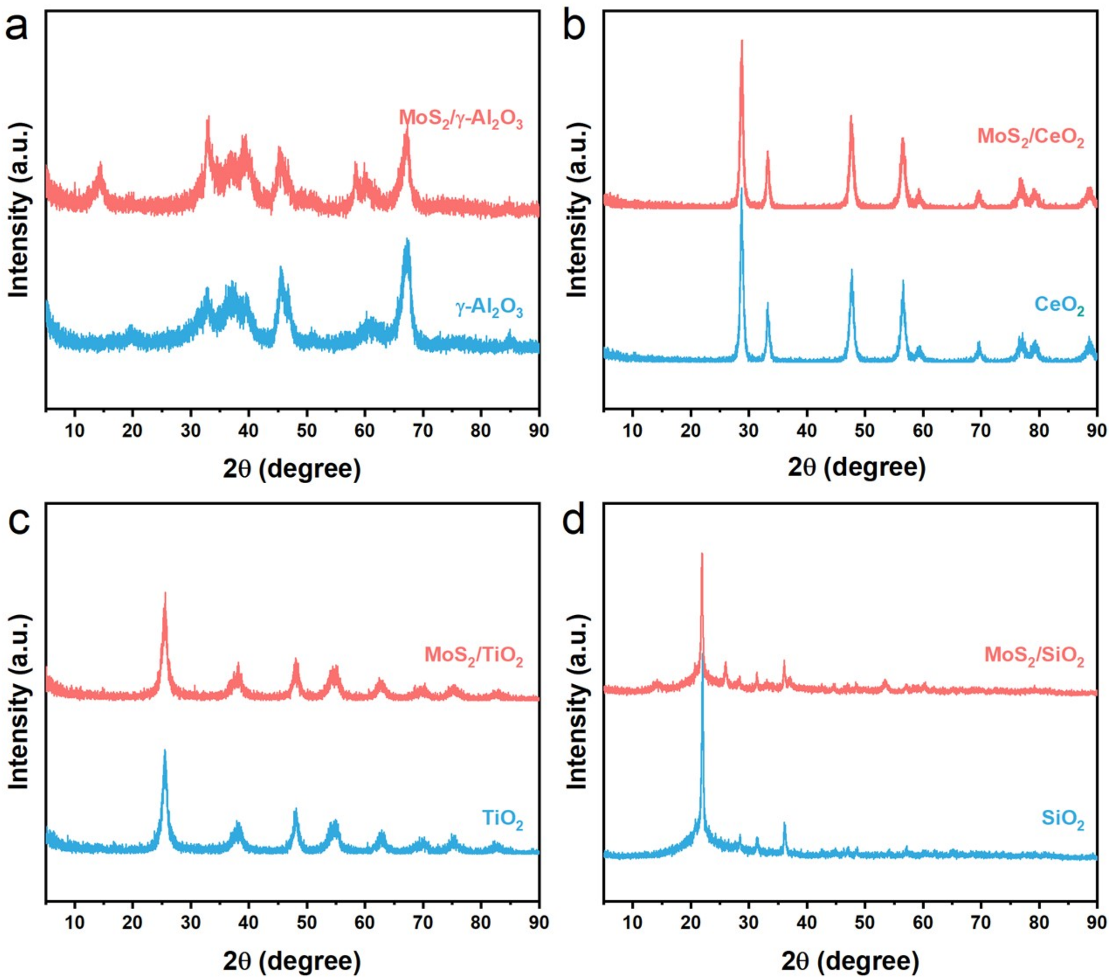

Fig. S4 XRD patterns of different support materials and their corresponding MoS_2-loaded catalysts. (**a**) γ-Al_2O_3 and MoS_2/ γ-Al_2O_3. (**b**) CeO_2 and MoS_2/CeO_2. (**c**) TiO_2 and MoS_2/TiO_2. (**d**) SiO_2 and MoS_2/SiO_2.

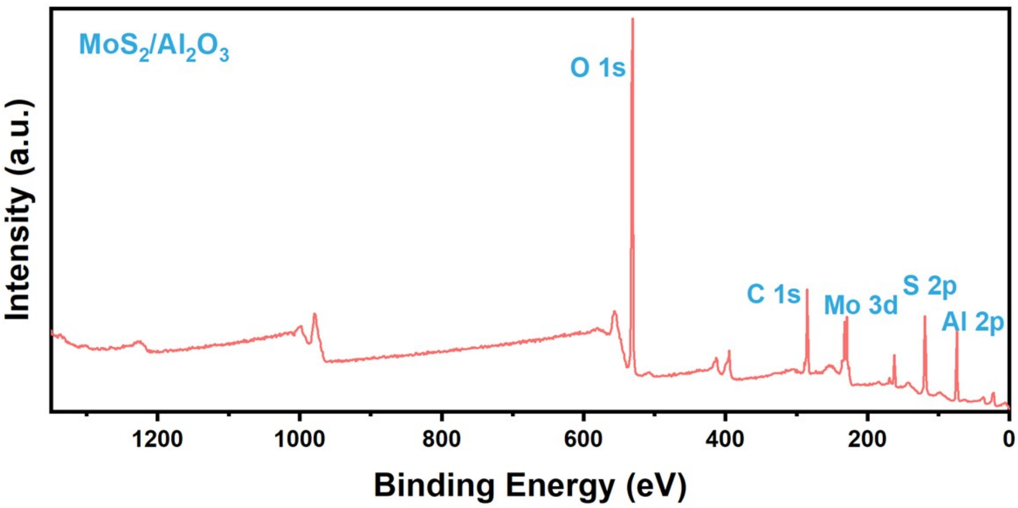

Fig. S5 XPS survey spectrum of the MoS_2/Al_2O_3 catalyst.

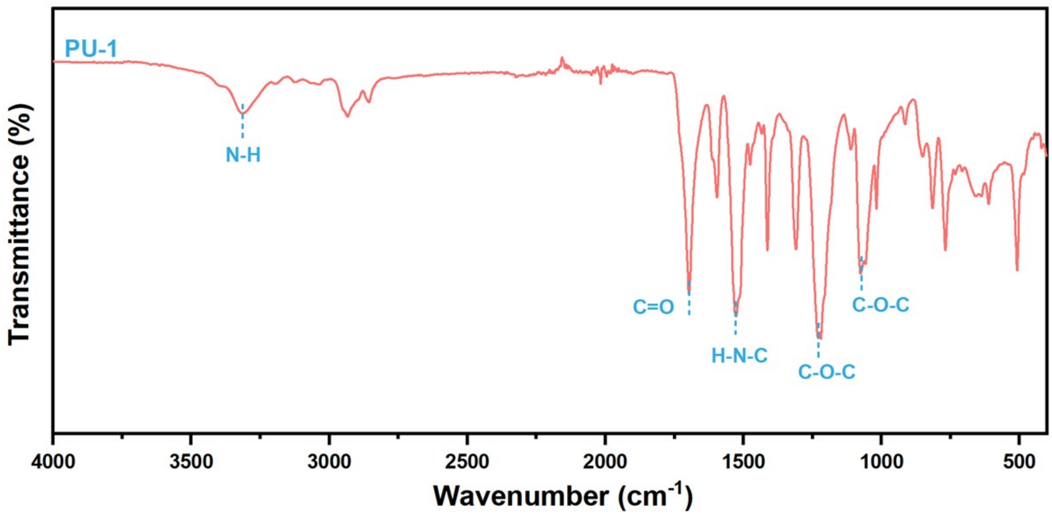

Fig. S6 FT-IR spectrum of **PU-1**.

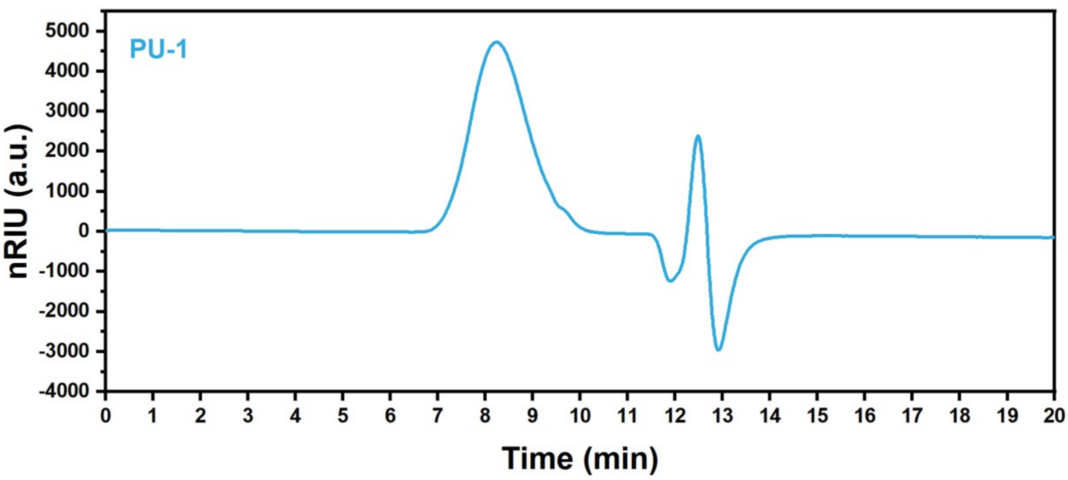

Fig. S7 GPC chromatogram of **PU-1**.

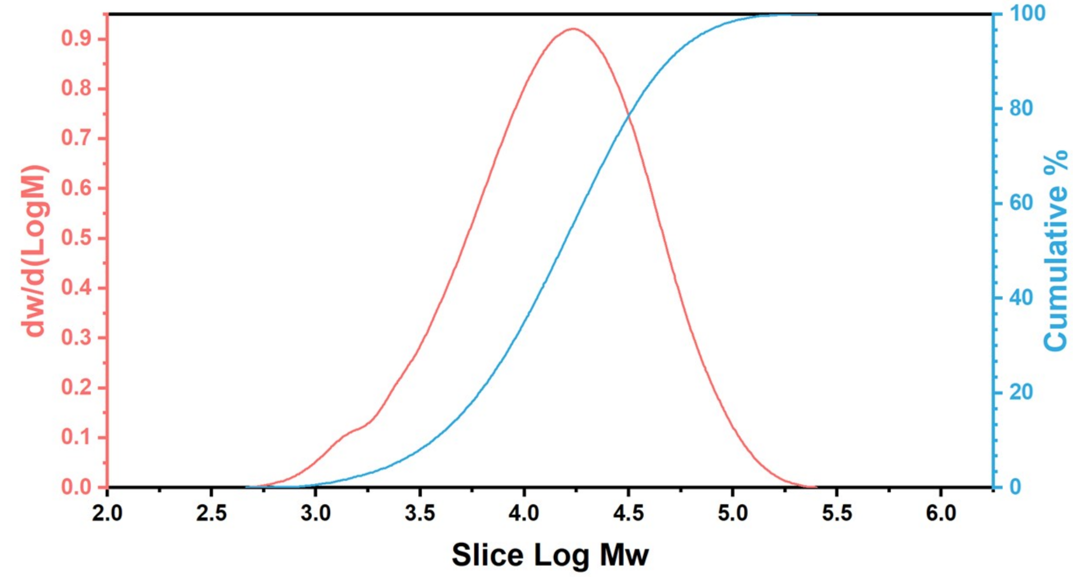

Fig. S8 Molecular weight distribution of **PU-1** (GPC).

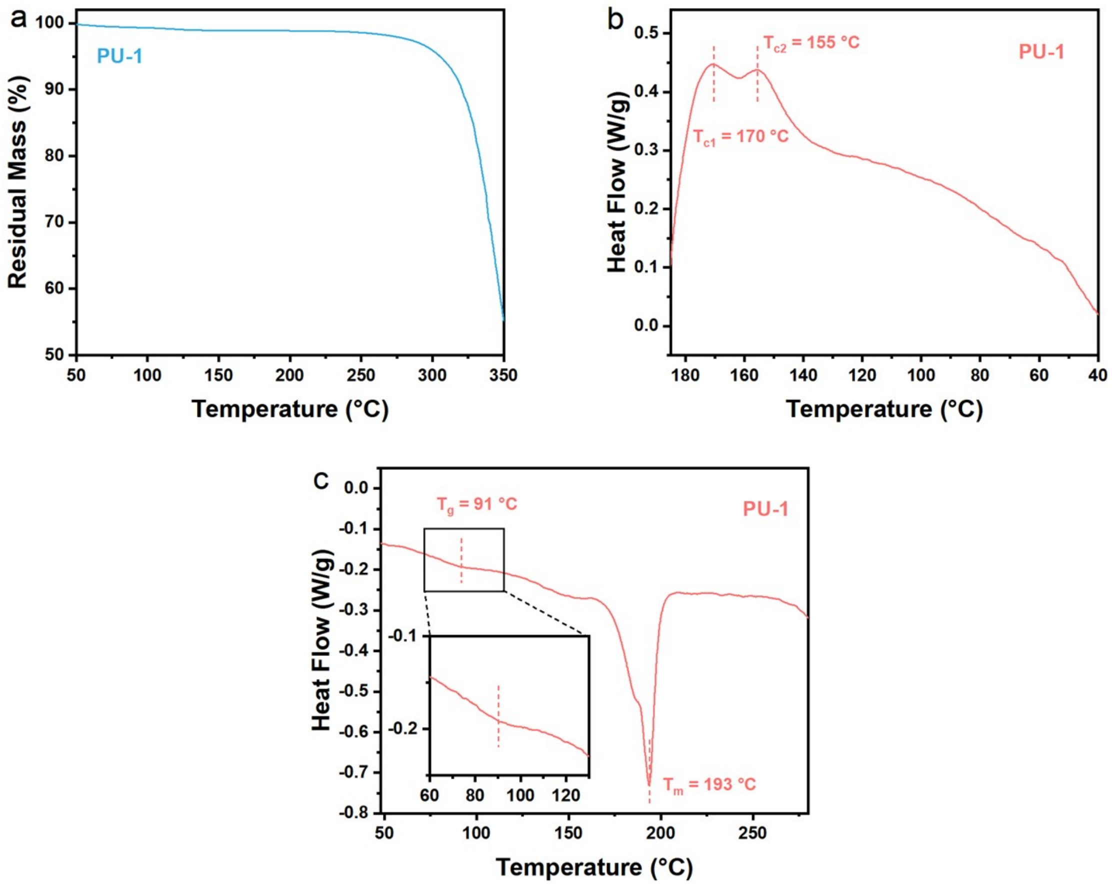

Fig. S9 TGA curve **(a)** and DSC curve **(b, c)** of **PU-1**. The DSC measurement was conducted as follows: heating from 30 °C to 185 °C at 10 °C min^{-1}, holding for 5 min; then cooling to 30 °C at 5 °C min^{-1}, holding for 15 min; and finally heating to 280 °C at 10 °C min^{-1}.

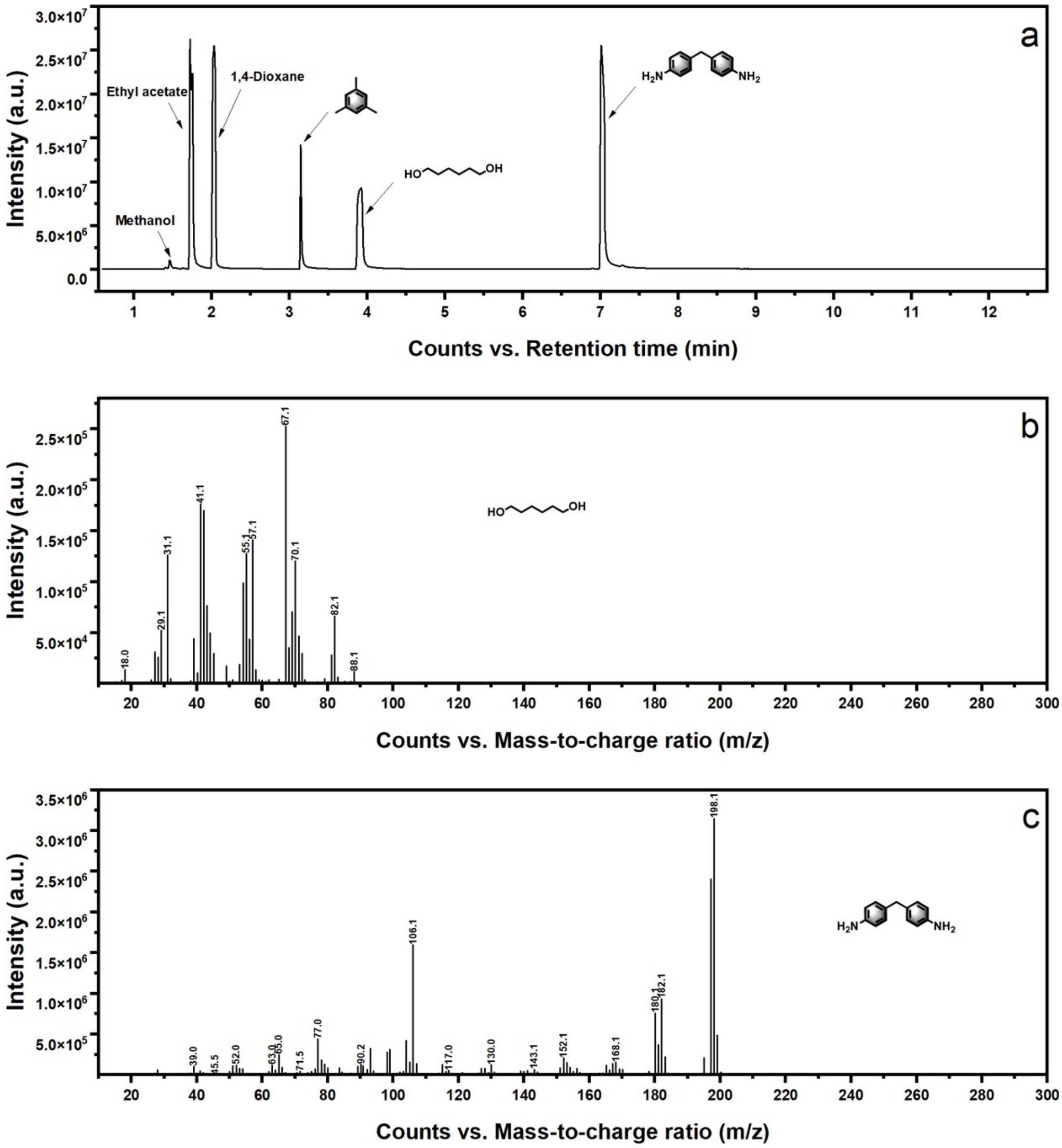

Fig. S10 GC-MS chromatogram **(a)** and mass spectra **(b, c)** of the products from **PU-1** hydrogenation. Reaction conditions: 300 mg of **PU-1**, 50 mg of MoS_2/Al_2O_3 catalyst, 15 mg of K_2CO_3, 5 mL of 1,4-dioxane, 185 °C, 5 MPa of H_2, 12 h, and stirring at 600 rpm.

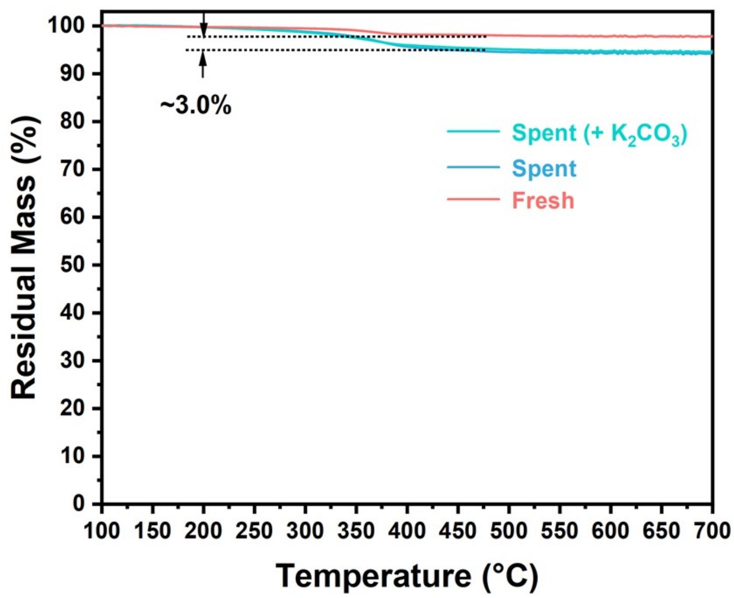

Fig. S11 TGA curves of the fresh, spent, and spent (with K_2CO_3 additive) MoS_2/Al_2O_3.

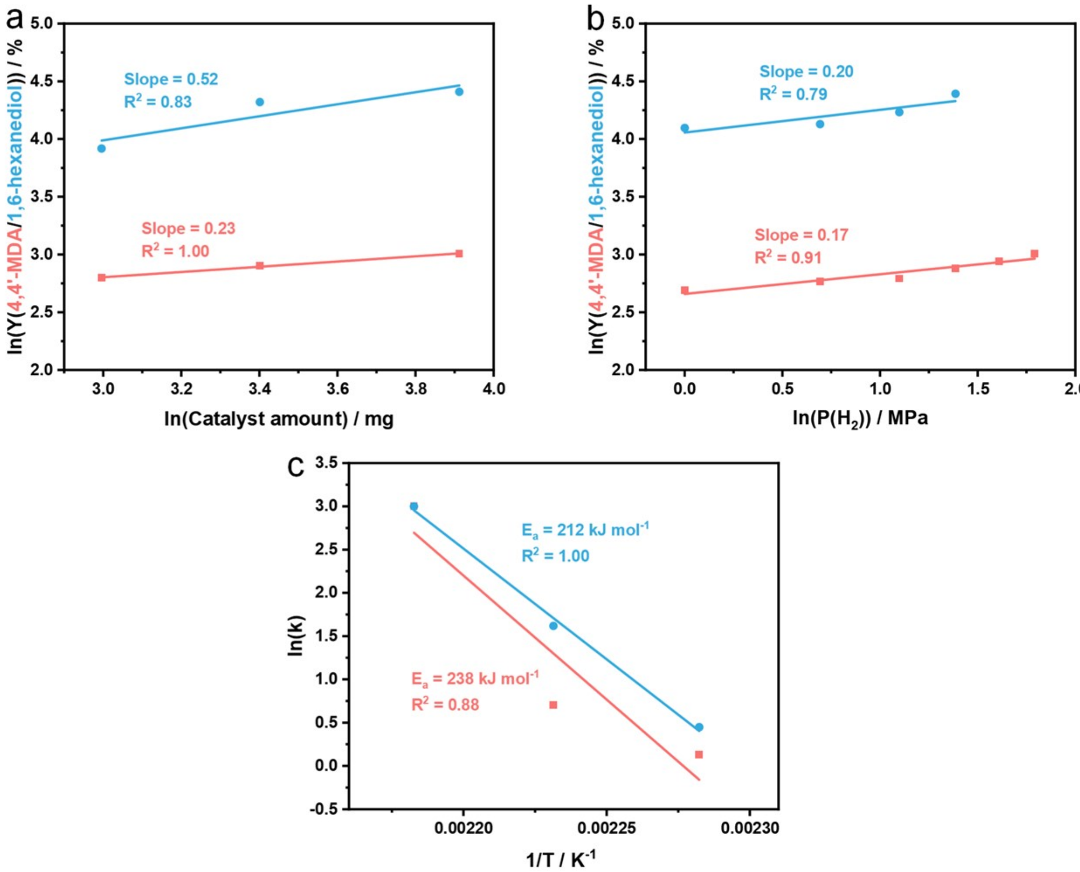

Fig. S12 (a) Linear fitting for the apparent reaction order with respect to catalyst amount for 4,4'-MDA and 1,6-hexanediol. (b) Linear fitting for the apparent reaction order with respect to H_2 pressure for 4,4'-MDA and 1,6-hexanediol. (c) Arrhenius plot for the apparent activation energy of 4,4'-MDA and 1,6-hexanediol.

Note: Owing to the lack of a well-defined substrate concentration for PU, product yield was used instead of conversion for the apparent kinetic calculations. The apparent rate equations are expressed as follows: for 4,4'-MDA, $r_1 = A_1\exp(-238000/(8.314T))(\text{catalyst amount, mg})^{0.23}(P(H_2, \text{MPa}))^{0.17}$; for 1,6-hexanediol, $r_2 = A_2\exp(-212000/(8.314T))(\text{catalyst amount, mg})^{0.52}(P(H_2, \text{MPa}))^{0.20}$. Herein, A_1 and A_2 are the pre-exponential factors for 4,4'-MDA and 1,6-hexanediol, respectively; 8.314 is the universal gas constant ($J\cdot mol^{-1}\cdot K^{-1}$); T is the absolute temperature (K); the units of activation energy are $J\cdot mol^{-1}$, the catalyst amount is mg, and the H_2 pressure is MPa. The rate-determining step (RDS) for 4,4'-MDA formation is the catalytic cleavage of the urethane C–N bond in PU. In contrast, RDS for 1,6-hexanediol formation is associated with the adsorption/activation of H_2 on the catalyst surface.

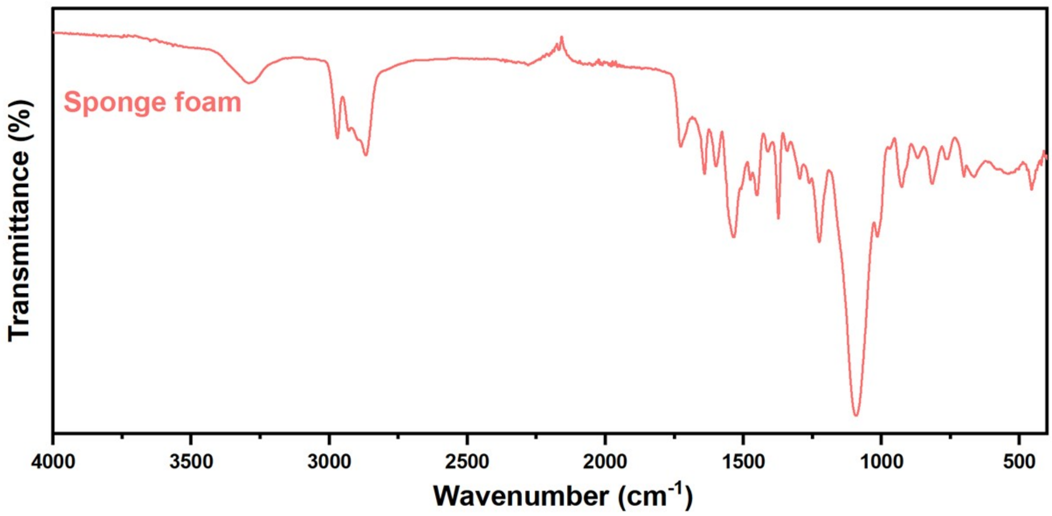

Fig. S13 FT-IR spectrum of sponge foam.

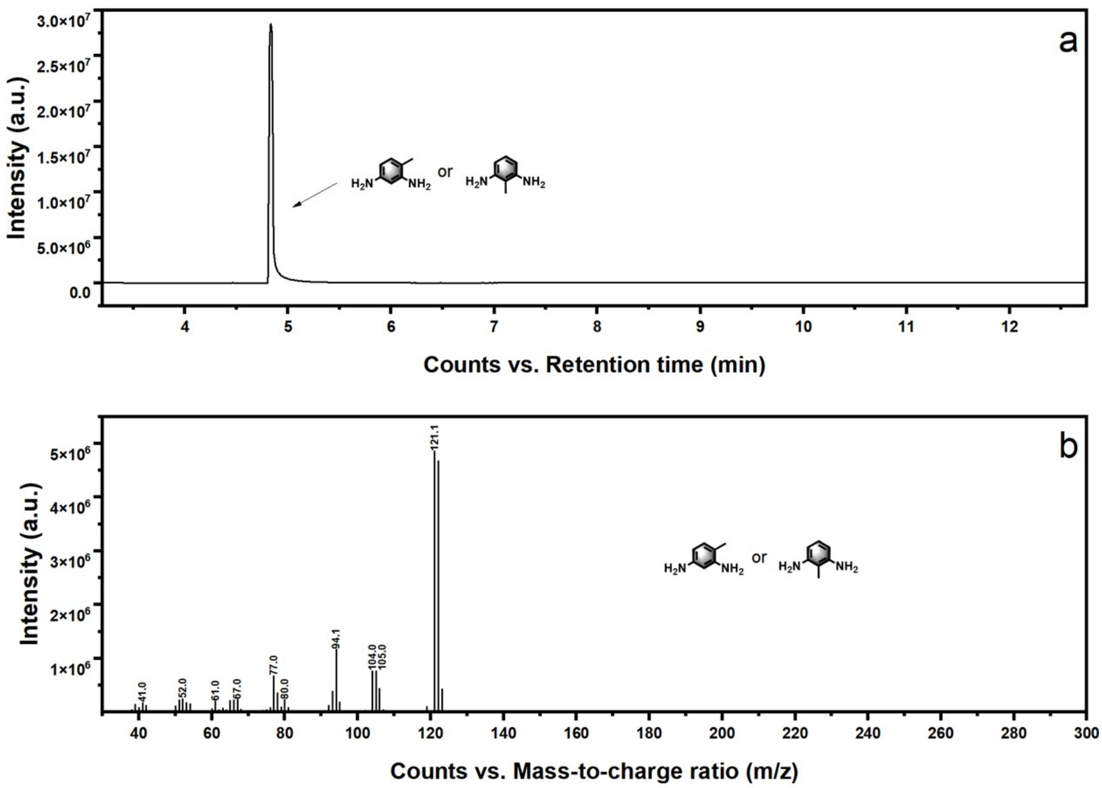

Fig. S14 GC-MS chromatogram **(a)** and mass spectra **(b, c)** of the products from sponge foam hydrogenation. Reaction conditions: 2500 mg of sponge foam, 420 mg of MoS_2/Al_2O_3, 175 mg of K_2CO_3, 10 mL of 1,4-dioxane, 190 °C, 7 MPa of H_2, 20 h, and stirring at 600 rpm.

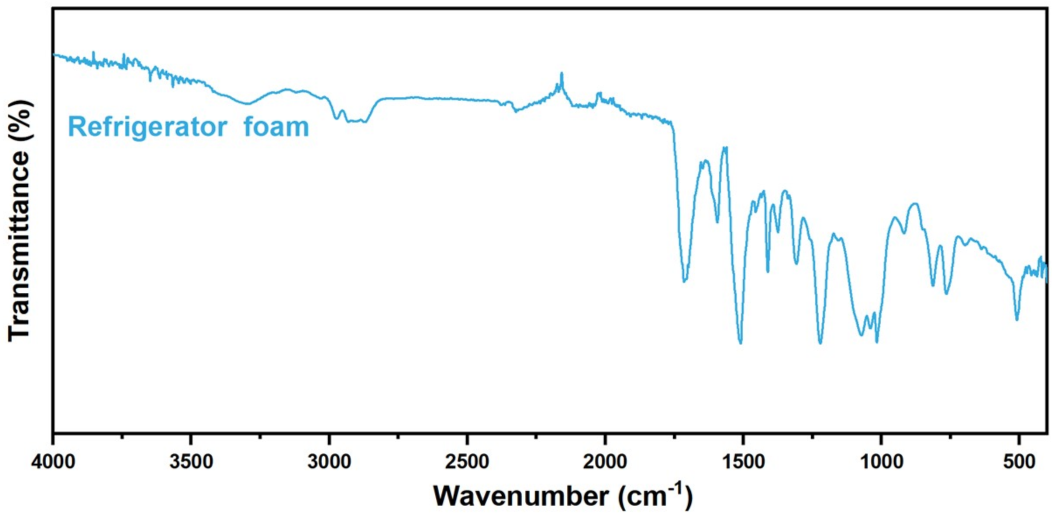

Fig. S15 FT-IR spectrum of refrigerator foam.

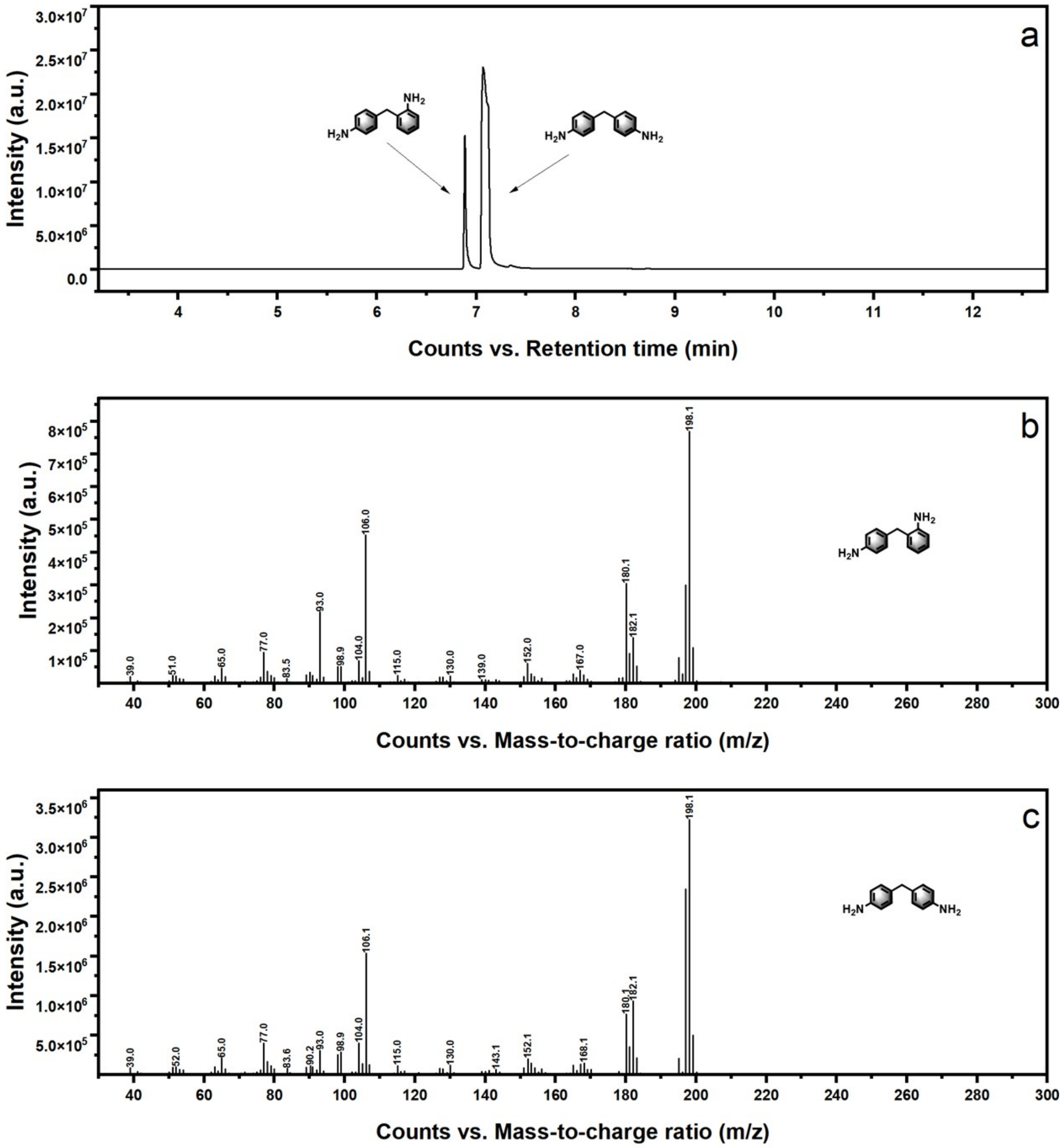

Fig. S16 GC-MS chromatogram **(a)** and mass spectra **(b, c)** of the products from refrigerator foam hydrogenation. Reaction conditions: 2500 mg of refrigerator foam, 420 mg of MoS_2/Al_2O_3, 175 mg of K_2CO_3, 10 mL of 1,4-dioxane, 190 °C, 7 MPa of H_2, 20 h, and stirring at 600 rpm.

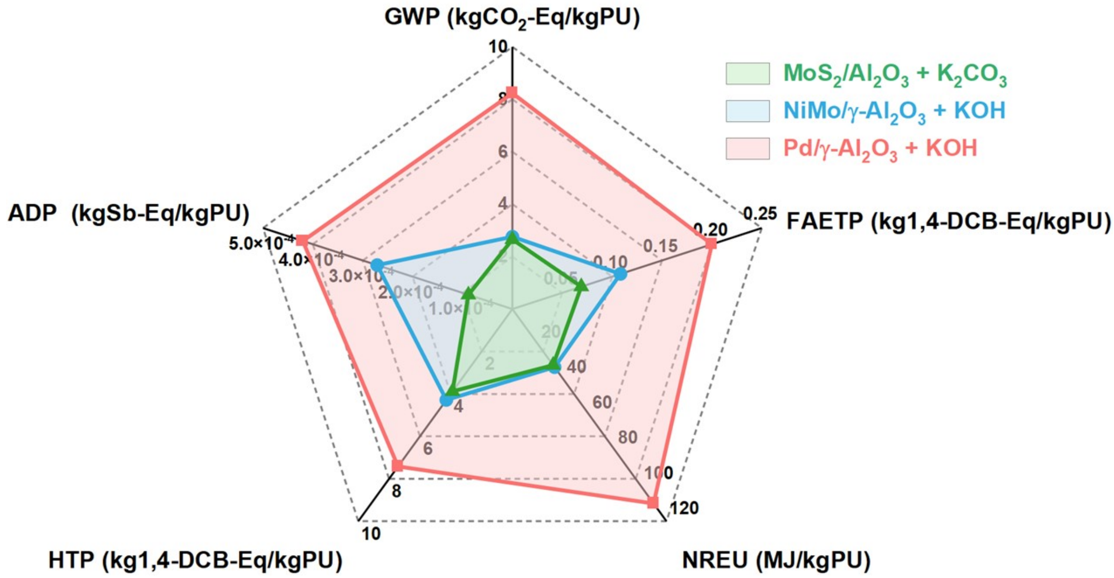

Fig. S17 Radar chart comparing the relative environmental impacts of three catalytic systems ($MoS_2/Al_2O_3 + K_2CO_3$, NiMo/γ-Al_2O_3 + KOH, and Pd/ γ-Al_2O_3 + KOH) across five LCA indicators: GWP, FAETP, NREU, HTP and ADP. Data correspond to Tables S5–7.

References

1 A. Kumar, N. von Wolff, M. Rauch, Y. Q. Zou, G. Shmul, Y. Ben-David, G. Leitus, L. Avram and D. Milstein, *J. Am. Chem. Soc.*, 2020, **142**, 14267-14275.

2 W. Zhou, P. Neumann, M. Al Batal, F. Rominger, A. S. K. Hashmi and T. Schaub, *ChemSusChem*, 2021, **14**, 4176-4180.

3 L. Gausas, S. K. Kristensen, H. Sun, A. Ahrens, B. S. Donslund, A. T. Lindhardt and T. Skrydstrup, *JACS Au*, 2021, **1**, 517-524.

4 X. Liu and T. Werner, *Chem. Sci.*, 2021, **12**, 10590-10597.

5 V. Zubar, A. T. Haedler, M. Schütte, A. S. K. Hashmi and T. Schaub, *ChemSusChem*, 2022, **15**, e202101606.

6 L. Gausas, B. S. Donslund, S. K. Kristensen and T. Skrydstrup, *ChemSusChem*, 2022, **15**, e202101705.

7 Z. Wang, X. L. Yan, N. Ma, S. Liu, P. Han, H. L. Li, Q. Mahmood, L. B. Li and Q. B. Liu, *J. Catal.*, 2023, **428**, 115165.

8 B. Sun, J. W. Zou, W. J. Qiu, S. H. Tian, M. L. Wang, H. Y. Tang, B. T. L. Wang, S. F. Luan, X. Y. Tang, M. Wang and D. Ma, *Natl. Sci. Rev.*, 2025, **12**, nwae393.

9 W. Q. An, X. Liu, X. D. Zhang, R. T. Gao, Z. J. Chen, Y. D. Hou and H. Du, *ChemSusChem*, 2025, **18**, e202402321.

10 X. B. Wu, R. C. Turnell-Ritson, P. J. Han, J. C. Schmidt, L. Piveteau, N. Yan and P. J. Dyson, *Nat. Commun.*, 2025, **16**, 4322.

11 B. Sole, J. S. Kolb, R. Marcial-Hernandez, J. Luk, T. Williams, O. V. Magdysyuk, D. Sheppard, G. Walker and A. Kumar, *ACS Sustainable Chem. Eng.*, 2025, **13**, 17173-17181.